Engineering with Computers (2020) 36:325–344
https://doi.org/10.1007/s00366-019-00702-7

ORIGINAL ARTICLE

A predictive model based on an optimized ANN combined with ICA for predicting the stability of slopes

Wei Gao[1] · Mehdi Raftari[2] · Ahmad Safuan A. Rashid[3] · Mohammed Abdullahi Mu'azu[4] · Wan Amizah Wan Jusoh[5]

Received: 5 December 2018 / Accepted: 2 January 2019 / Published online: 4 February 2019

Abstract

In this study, we optimized artificial neural network (ANN) with imperialist competition algorithm (ICA) for the problem of slope stability design charts. To prepare training and testing datasets for the ANN and ICA–ANN predictive models, an extensive number of limit equilibrium analysis modelings (e.g., for the lower bound, LB, limit analysis and upper bound, UB, limit analysis) was conducted. The analyses were conducted using OptumG2 computer software and implemented on two-layered cohesive soil layer sets. For each of the LB and UB limit analysis, the database consisted of 320 training datasets and 80 testing datasets. Variables of the ICA algorithm such as the number of countries, the number of initial imperialists and the number of decades were optimized using a series of trial-and-error process. The input parameters that used thorough the OptumG2 finite element modeling (FEM) analysis include depth factor (i.e., the ratio of first soil layer thickness to the slope height), slope angle, undrained shear strength ratio where the output was taken dimensionless stability number. The estimated results for both of datasets (e.g., training and testing) from ANN and ICA–ANN models were assessed based on three known statistical indices namely value account for (VAF), root means squared error (RMSE), and coefficient of determination (R^2). To evaluate the performance of proposed models, color intensity rating (CER) and total ranking method (TRM), i.e., based on the result of statistical indices, was used. After 72 trial-and-error processes (e.g., sensitivity analysis on some neurons) the optimal architecture of $3 \times 6 \times 1$ were found for both of the ANN–UB and ANN–LB models. As a result, both models presented excellent performance, however according to the introduced ranking system the ICA–ANN model could slightly perform a better performance compared to ANN. Based on R^2, RMSE and VAF values of (0.9999, 0.0107 and 99.9924) and (0.9991, 0.0102 and 99.9913), respectively, were found for training and testing of the optimized ICA–ANN–LB predictive model. Similarly, for the ICA–ANN–UB predictive model, values of (0.9984, 0.0129 and 99.9659) and (0.9984, 0.01047 and 99.9915) were obtained for the R^2, RMSE and VAF of training and testing datasets, respectively. However, in the ANN model, the R^2 and RMSE for both of the training and testing datasets were (0.9982 and 0.01815) and (0.9972 and 0.01748), respectively. This proves a better performance of the ICA–ANN model in predicting the behaviors of slope stability of cohesive soils and consequently more reliable design solution charts provided herein.

Keywords ANN · ICA–ANN · Optimization · Slope stability · Design charts

✉ Wei Gao
gaowei@ynnu.edu.cn

[1] School of Information Science and Technology, Yunnan Normal University, Kunming, China

[2] Department of Civil Engineering, Khorramabad Branch, Islamic Azad University, Khorramabad, Iran

[3] Centre of Tropical Geoengineering (Geotropik), School of Civil Engineering, Faculty of Engineering, Universiti Teknologi Malaysia, Johor Bahru, Malaysia

[4] Department of Civil Engineering, Jubail University College, Royal Commission of Jubail and Yanbu, Jubail 31961, Kingdom of Saudi Arabia

[5] Faculty of civil engineering and environment, Universiti Tun Hussein Onn Malaysia, Parit Raja, 86400 Batu Pahat, Johor Darul Takzim, Malaysia

1 Introduction

Calculation of the slope stability has always been one of the important tasks for all civil engineers. This concern can be mentioned for cut slopes, natural slopes or human-made filled slopes (e.g., earth dams, levees, and embankment) [1–5]. Sometimes the slope consists of several soil layers resting on a rigid bedrock. In particular slopes, there are various parameters such as soil properties, geology, and hydrology that will affect the factor of safety (FS) [6, 7]. Many studies are conducted in order to improvise the way that engineers will assess the slope stability [8–10]. One of the easiest solutions for designers is to use the design solution charts in which they can have a proper approximation according to the origin of their problems [6, 7, 9, 11]. Several researchers provided slope stability design charts based on traditional methods of slope stability analysis (e.g., [4, 12]). Most traditional methods rely on simplified solutions, i.e., using linear analysis consideration and extensive experimental methods [10, 13]. As an easy solution, the earliest slope stability design chart developed by Taylor [14]. These simply designed charts were extensively used through the slope stability analysis for decades. By advancing mathematical solution and engineering computer software, more sophisticated numerical modeling was conducted on the problem of slope stability. It is well established that the artificial neural network (ANN) can be used to approximate (e.g., to any desired degree of accuracy) any continuous function. The main advantage of ANN is that it can utilize any required number of neurons and that it is endowed with a limited number of hidden layers [15]. Also, for implementing the ANN, there is no prior knowledge of the data generating process required. Many types of research have proved that the ANNs are reliable methods for approximating the slope stability analysis (e.g., [16–18]).

In contrast, there are several problems of using ANN models such as being trapped in their local minima and slow rate of the learning system. Moreover, the addition of hidden layers will lead to overfitting the trained network. This can be seen when the model trained very well, however, the testing dataset of the ANN will generate inferior results in case of predicting the selected samples [19–21]. Note that finding and building up the optimized ANN architecture is time-consuming and requires a long trial-and-error activity. In recent years, new examples of optimizing ANN with optimization algorithms such as genetic algorithm (e.g., [22, 23]), particle swarm optimization algorithm (e.g., [24, 25]) and imperialist competition algorithm (ICA) (e.g., [26]) are used to estimate different engineering design parameters. In this regard, the use of an optimization algorithm in the assessment of slope stability design solution charts is yet to be discovered.

Due to time and cost constraints especially in complex problems, providing numerical analysis is not always feasible and warranted. Hence, the easiest solution for engineering application is to use a solution design slope stability chart. There are very few studies on the use of ANN-based models on the problem of slope stability (e.g., [27–29]). The hybrid ICA–ANN models presented here are not used in the problem of slope stability and also it can be carefully highlighted as a new topic in most civil engineering applications. There is almost no study performed on the use of hybrid ICA–ANN-based learning systems (e.g., to predict the safety factor of slope) and its influential parameters. In this study, to predict the behaviors of slope stability of two-layered cohesive slope (i.e., factor of safety) subjected to its natural soil weight (e.g., surcharge is not included), 72 different ANN models (six iterations based on different number of neurons and finite element analysis type) and 29 hybrid ICA optimized with artificial neural network (ICA–ANN) models were designed. All the proposed models were evaluated with the use of a trial-and-error process and their influential parameters were assessed (e.g., to search for the optimal set of parameters setting). In this regard, based on the suggestion from other studies (e.g., [2, 30–34]), the influential parameters that will affect the stability of a two-layered cohesive slope are taken as input parameters (e.g., soil layer thickness (d), the slope height (h), slope angle (β), undrained shear strength ratio of upper soil layer C_{u1}) undrained shear strength of lower soil layer (C_{u2}) where the output was taken a dimensionless stability number (N_{2c}). Therefore, the main objective of this study is to optimize hybrid ANN models with ICA optimization algorithms for predicting N_{2c} and consequently the slope stability design solution charts for a purely cohesive soil.

2 Artificial intelligent systems

2.1 Artificial neural network

The ANN is firstly presented by McCulloch and Pitts [35]. There are several rules in ANN based on hypothesis and observations of neuro-physiologic nature. Many scholars have examined the expansion of simple and non-linear mathematical solutions based on the human biological neuron. These investigations lead to generating a large number of network learning algorithms (e.g., [22, 36–38]). ANN-based models process the database in a training network and assess the predicted output with a testing dataset. The ANN can be developed to solve the complex problems, almost in every discipline. This technique is known to be a multilayer structure that is extremely connectionist systems. During the training process of the network, it is able to learn tasks as well as recognize similarities with no pre-defined programming. The learning system is normally without any prior information about the problems, e.g., different inputs parameters that were set in the input dataset layers. Instead, the ANN automatically develops identifying features from the learning material (e.g., input and output datasets) that they process. The three main parts of the ANN model structure consists of (1) input, (2) hidden and (3) output layers. For a given problem the ANN uses three main components namely, (1) transfer function (e.g., a continuous, monotonically increasing, differentiable function, employed to the weighted input of a neuron to generate the final output); (2) network architecture (e.g., outline for the requirement of a network's components and their functional configuration), and (3) learning law (e.g., mathematical algorithms applied to the neural network's connection weights on how to change right after each learning step). These components are considered in order to select the most appropriate model for a given problem(s). Note that one of the ANN capability is to extract the existing equations between the several input dataset variables and the output. This can be done through the usage of an appropriate learning method. After the learning process, the proposed network can simply generalize the acquired knowledge to predict the real output with an acceptable degree. In another word, the developed networks enable to predict the values for an unknown output. To assess the validity of the methods, calculation of the error is conducted based on a comparison between the predicted output (generated output) and the targets (desired output). To assess the network outputs different statistical indexes can be used namely, variance-account-for (VAF), root mean squared error (RMSE) and coefficient of determination (R^2). For example, in cases where VAF and R^2 are higher than the calculated error, the stopping criteria did not meet, hence, the network will back-propagate and set a new connection weight till it can meet the termination criteria. Figure 1 demonstrates the details of most common ANN algorithms.

2.2 Imperialist competitive algorithm (ICA)

ICA is one of the optimization algorithms that has been widely used thorough literature (e.g., [39]). This optimization algorithm firstly suggested by Atashpaz-Gargari and Lucas [40]. ICA is a system that search population similar to many other evolutionary algorithms (e.g., genetic algorithm, evolutionary programming, gene expression programming). ICA gets started with a given population by users (e.g., consists of countries defined initially). The pre-defined countries are separated into two groups: (1) the first group is called Imperialists consists of some of the best countries among the pre-defined populations and (2) the second group that is called Colonies which is the rest of countries that left to be involved in the first group (see Fig. 2). In order to generate empires, the colonies (e.g., second group) are divided among the imperialists (e.g., first group). This distribution is determined by a series of pre-defined criterion and it can be done based on each colony's relative strength. Next, the empires (i.e., that have a number of colonies) try to expand their territories (i.e., become more powerful) by controlling more colonies. This can be done by competing with other empires. As a result of these competitions, the strongest empire could take possession of smaller (i.e., weaker) colonies. The process stopped when the pre-defined stopping criterion is satisfied. The learning and optimization process of the ICA algorithm alone is well described in other studies (e.g., [31, 41]).

2.3 Combination of ICA–ANN

There have been many investigations to increase the performance of ANN predictive models using optimization algorithms. Some of the well-known optimization algorithms are ICA, GA, and PSO. These algorithms can help engineers to find a more reliable solution for any engineering problems. Since backpropagation-based algorithms are known as a local learning algorithm search system, the optimal (e.g., with the pre-defined structure that can be obtained based on trial and error) search learning process of ANN may not be

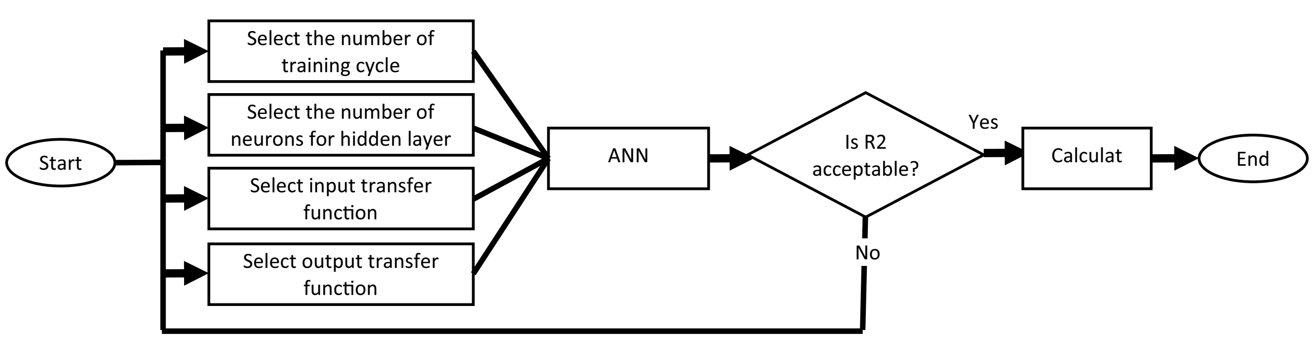

Fig. 1 A general flowchart for the ANN models

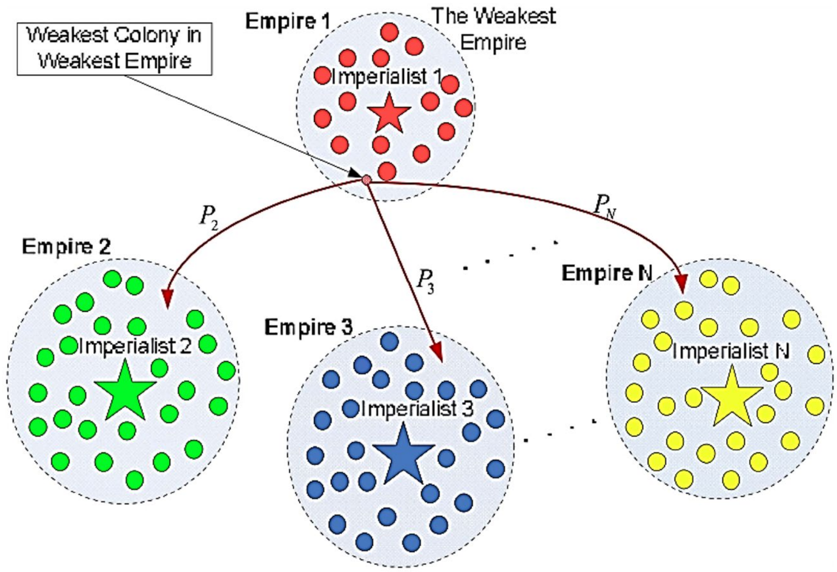

Fig. 2 Taking possession of the weakest colony during the imperialistic competition (e.g., after Atashpaz-Gargari and Lucas [40])

able to provide an unsatisfied solution [42]. In this regard, optimization algorithms can be utilized to optimize the values of weight and bias of the ANN. Hence the level of error rate will reduce and consequently the performance level will increase. In addition, to find the local minimum in any ANN system, there is a higher probability of convergence since optimization algorithms can accurately find the global minimum. Therefore, as the main priority of hybrid ICA–ANN model is its searching properties, it can benefit from using both the ANN as well as the ICA techniques. For instance, in searching for a reliable learning system (e.g., to search for the weights and bias), the hybrid optimization algorithm of ICA will look after for the global minimum while the ANN model helps to find the lowest error for the system (i.e., best results of the system).

3 Problem definition and data collection

As stated earlier the slope stability of cohesive soil layers is crucial in most engineering projects. The calculation of slope stability, however, is a difficult task and can be costly as well as time-consuming. Therefore, this study focused on providing design solution charts for a cohesive slope (e.g., with a maximum of two layers in each example). Conventional methods of slope analysis used extensively since the 1930s where the first design charts are provided by Taylor [14]. Developing advanced design tools, i.e., using optimization algorithms as well as ANN-based predictive models, draw the attention of many researchers. However, most ANN training models have problems in their learning systems. These problems, i.e., that lead to the low performance of ANN results, can be solved by using optimization algorithms such as ICA. Existing applications of ICA predictive models to ANN training networks have not been used in the area of slope stability; neither measure the important factors influencing this problem nor the optimal architecture of the network. Therefore, the main objective of this paper is to propose a new hybrid ICA-based ANN model to predict dimensionless stability number (N_{2c}).

This study employs a lower bound (LB) limit analysis (e.g., as suggested by Sloan [43], Zhou et al. [44] and Lim et al. [45]) and upper bound (UB) limit analysis (e.g., as suggested by Donald and Chen [32], Chen et al. [46], Chen et al. [47] and Zhao et al. [48]) to assess the short-term stability of slopes in which the subgrade foundation and slope materials have two separated cohesive materials (i.e., having only undrained shear strengths). The analysis is conducted with OptumG2 computer software. This computer software is a comprehensive finite element program that has been recently developed for deformation analysis and geotechnical stability problems [49] and widely used in other studies (e.g., [50–52]). To simplify the stability problem, the analysis is conducted using the plane-strain cases (e.g., three-dimensional boundary condition was not considered as the third dimensions assumed to have no effect in the 2D limit analysis).

The description of the problem studies herein is shown in Fig. 3. To provide the design solution charts using ICA–ANN and ANN techniques, the first need is to provide a useful slope geometry. The sloping geometry consists of two purely cohesive soils (i.e., having only undrained cohesive strength, C_{u1}). The cohesion in the top and bottom soil layers is taken C_{u1} and C_{u1}, respectively. These two soil properties can be different. Note that the analysis is performed with different slope height (H), undrained shear strength and thickness of both soil layers (d). Graphical summary of the range of input data versus

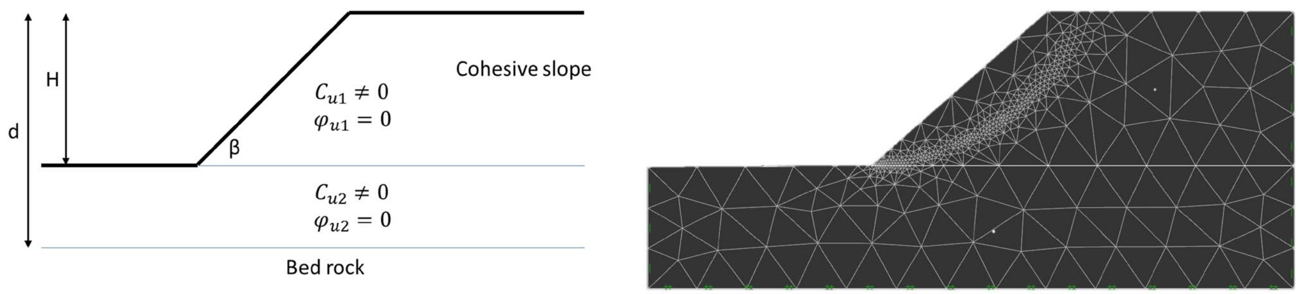

(a) schematic model, **(b)** OptumG2 model

Fig. 3 A view of the model for the two-layered cohesive slope

dataset number for *d*/*H* ratio, slope angle, and C_{u1}/C_{u2} is illustrated in Fig. 4a–c, respectively. In this regard and for the case of this research, the database used to train the models was obtained from a total of 800 full-scale (i.e., for both of the UB and LB limit analysis) simulations. The obtained results from 320 (e.g., for each one of the UB and LB limit analysis) OptumG2 calculations were chosen randomly to train the ANN network. In order to test and validate the network, 20% of the database (e.g., 80 cases for each of the testing and validation dataset) was selected. The database was provided for a two-layered cohesive slope rested on rigid bedrock.

4 Model development for prediction of N_{2c}

Development of a proper hybrid ANN model requires several phases such as, pre-processing (e.g., finding optimal parameters for the main inputs from the ANN predictive model) and normalization of the available data (e.g., this is not, however,

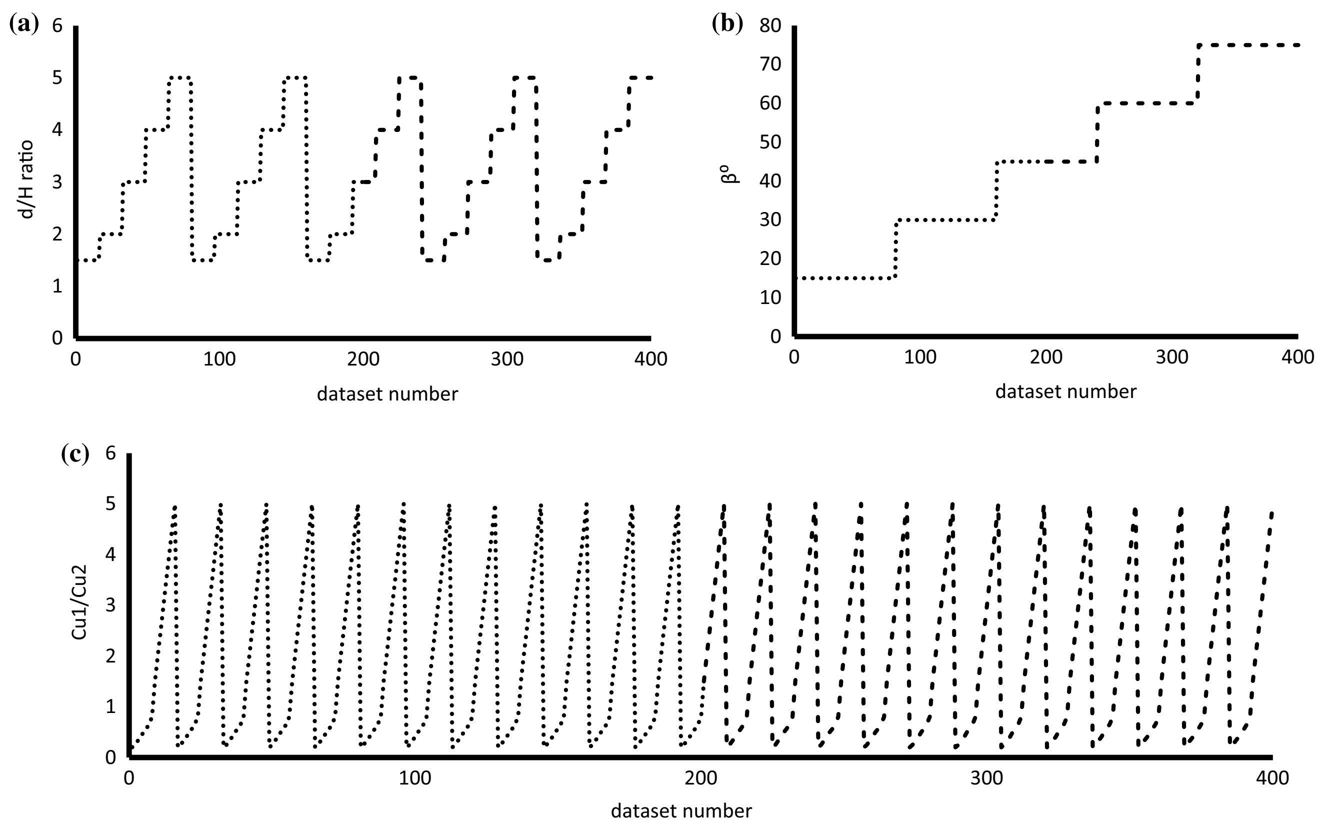

Fig. 4 Graphical summary of the range of input data versus dataset number for **a** *d*/*H* ratio, **b** slope angle, **c** C_{u1}/C_{u2}

a mandatory task and the data can be used without any normalization), finding of a reliable predictive hybrid model (e.g., finding a proper hybrid model and its optimization) to train input and output(s) datasets in order to train a good network, and the last phase which is determination of a suitable hybrid network architecture (e.g., using a trial and error and parametric study on the influential parameters of each model). The input datasets include (1) depth factor, d/H, (ratio of first soil layer thickness, d, to the slope's top layer height, H); (2) undrained shear strength ratio (C_{u1}/C_{u2}) and (3) slope angle (β) where the output was taken N_{2c}. Note that to present a non-normalized version of the predicted results (e.g., required for the design chart solutions, N_{2c} proposed by Taylor [14]) was defined in Eq. (1):

$$N_{2c} = C_{u1}/\gamma H F_s, \tag{1}$$

where F_s is the safety factor obtained from the OptumG2 simulation, γ is the soil unit weight which is taken 20 kN/m^3, C_{u1} is the undrained shear strength of so the top layer, and N_{2c} is dimensionless stability number.

An example of input and output dataset obtained from the OptumG2 simulation and effective parameters influencing the N_{2c}, as the model output, employed in ANN modeling is shown in Table 1. Note that the data were taken randomly from the data training input only.

Table 1 Example of inputs and output dataset applied for modeling purpose

Model number	Input			N_{2c} value		
				Measured output	Predicted output	
	d/H ratio	$\beta°$	C_{u1}/C_{u2}		ANN	ICA–ANN
1	1.5	15	0.2	0.0855	0.0881	0.0865
2	1.5	15	0.25	0.0855	0.0878	0.0901
3	1.5	15	0.33	0.0855	0.0891	0.095
4	1.5	15	0.4	0.0855	0.0906	0.0996
5	1.5	15	0.5	0.0855	0.0946	0.1056
6	1.5	15	0.57	0.0855	0.0977	0.1102
7	1.5	15	0.66	0.09025	0.1033	0.1158
8	1.5	15	0.8	0.1045	0.1149	0.124
9	2	15	0.2	0.0855	0.082	0.0921
10	2	15	0.25	0.0855	0.0809	0.0964
11	2	15	0.33	0.0855	0.0827	0.1027
12	2	15	0.4	0.0855	0.0845	0.1084
13	2	15	0.5	0.0855	0.0903	0.1162
14	2	15	0.57	0.0893	0.0939	0.122
15	3	15	3.5	0.4522	0.4783	0.5005
16	3	15	4	0.49875	0.5295	0.555
17	3	15	4.5	0.5434	0.5727	0.606
18	3	15	5	0.5852	0.6046	0.6534
19	4	15	0.2	0.0855	0.0956	0.038
20	4	15	0.25	0.0855	0.094	0.0458
21	4	15	0.33	0.0855	0.0963	0.0592
22	5	15	3.5	0.53105	0.563	0.4894
23	5	15	4	0.59565	0.631	0.5459
24	5	15	4.5	0.65835	0.6923	0.6002
25	5	15	5	0.7201	0.7446	0.6517
26	1.5	30	0.2	0.1273	0.1336	0.1238
27	1.5	30	0.25	0.1273	0.133	0.1271
28	1.5	30	0.33	0.1273	0.1334	0.1318
29	5	30	4.5	0.6821	0.7192	0.6378
30	5	30	5	0.74765	0.782	0.6888
31	1.5	45	0.2	0.15865	0.1688	0.1561
32	1.5	45	0.25	0.15865	0.1683	0.1592
33	1.5	45	0.33	0.15865	0.1684	0.1636

5 Results and discussion

5.1 Optimal artificial neural network predicting N_{2c}

Approximation of the dimensionless stability number (N_{2c}) for a two-layered cohesive slope using hybrid ICA–ANN is the main objective of this study. Therefore, the most significant network parameters on the calculation of the N_{2c} (i.e., depth factor, slope angle and the ratio of cohesion strength in the top and bottom layers) were used through the FEM limit analysis modeling. In this step, to train the proposed ANN network, five different datasets were provided for both of the LB and UB analysis. The main objective of considering different iterations for both training and testing datasets was to find the best ANN predictive model. The selection of the optimal ANN model can be made based on their error rate or prediction performances. To develop the models, considering suggestions from previous studies (e.g., [19, 23, 53]), the training and testing datasets were selected randomly from 80% of the both LB and UB limit analysis output (320 datasets for the training datasets) and 20% (80 datasets for the testing datasets), respectively. Similar to other models provided in this study the ANN modeling needs to be presented in its optimal architecture with a well-organized structure. This can be done in terms of the number of neurons (or nodes) considered in each hidden layer as well as choosing of proper ANN learning algorithm [54]. For the purpose of ANN training network, in this study, the Levenberg–Marquardt backpropagation (simply called trainlm function) was used. This training and learning system algorithm is widely used in other studies (e.g., [55–57]). This learning system is of interest of researchers due to its less complexity. It is well established that the number(s) of neuron in the hidden layer is known to be the most critical feature in the progress of trainlm function (e.g., or in most ANN training functions). According to recommendation presented in other studies (e.g., [58]) and considering the number of datasets input parameters used in this study, the number of nodes in the hidden layer changed from 1 to 6. Therefore, 36 ANN-trainlm models were constructed for each of the limit analysis types. Finally, their network performances were evaluated in order to search their optimal performances. Each ANN model was iterated six times and the average results from this iteration are tabulated in Tables 2, 3, 4 and 5. Note that, a network output with the higher R^2 or lower RMSE values is considered to perform better. A new color intensity rating system (CER) was used. The CER ranks the values obtained for the above-mentioned indexes. More details on how the CER works can be found in other studies (e.g., [1, 41, 59]).

Table 2 Obtained results of R^2 for several ANN (LM) models with different hidden nodes for the LB limit analysis method

Nodes in the hidden layer	Network result																
	R^2																
	Iteration 1		Iteration 2		Iteration 3		Iteration 4		Iteration 5		Iteration 6		Average		Average Ranking		Total ranking
	TR1	TS1	TR2	TS2	TR3	TS3	TR4	TS4	TR5	TS5	TR6	TS6	TR	TS	TR	TS	
1	0.97110	0.97301	0.97170	0.96670	0.97382	0.96975	0.97081	0.97066	0.97167	0.95595	0.97131	0.97252	0.97174	0.96810	1	1	2
2	0.98942	0.98846	0.98543	0.97587	0.99101	0.99215	0.99010	0.98756	0.99556	0.99573	0.98784	0.99242	0.98989	0.98870	2	2	4
3	0.99402	0.99300	0.99850	0.99822	0.99814	0.99761	0.99698	0.99692	0.99761	0.99763	0.99766	0.99770	0.99715	0.99685	3	3	6
4	0.99722	0.99776	0.99928	0.99836	0.99881	0.99847	0.99820	0.99909	0.99919	0.99896	0.99935	0.99928	0.99867	0.99865	4	4	8
5	0.99944	0.99935	0.99925	0.99906	0.99915	0.99854	0.99949	0.99924	0.99946	0.99922	0.99752	0.99736	0.99905	0.99879	5	5	10
6	0.99936	0.99928	0.99923	0.99906	0.99934	0.99925	0.99926	0.99916	0.99973	0.99970	0.99958	0.99948	0.99942	0.99932	6	6	12

Higher intensity of colour means higher validity

Table 3 Obtained results of RMSE for 14 ANN (LM) models with different hidden nodes for the LB limit analysis method

Model number	Nodes in the hidden layer	Network result														Average Ranking		Total ranking
		RMSE																
		Iteration 1		Iteration 2		Iteration 3		Iteration 4		Iteration 5		Iteration 6		Average				
		TR1	TS1	TR2	TS2	TR3	TS3	TR4	TS4	TR5	TS5	TR6	TS6	TR	TS	TR	TS	
1	1	0.04479	0.03874	0.04440	0.04402	0.04494	0.04310	0.04494	0.04310	0.04370	0.05446	0.04306	0.04659	0.04431	0.04500	1	1	2
2	2	0.02721	0.02708	0.03200	0.03661	0.02642	0.02406	0.02642	0.02406	0.01740	0.01698	0.02821	0.02460	0.02628	0.02557	2	2	4
3	3	0.02034	0.02152	0.01016	0.01096	0.01256	0.01435	0.01256	0.01435	0.01249	0.01372	0.01268	0.01258	0.01346	0.01458	3	3	6
4	4	0.01353	0.01348	0.00720	0.00969	0.00907	0.00998	0.00907	0.00998	0.00762	0.00777	0.00660	0.00783	0.00885	0.00979	4	4	8
5	5	0.00649	0.00640	0.00720	0.00816	0.00829	0.00934	0.00829	0.00934	0.00607	0.00740	0.01293	0.01422	0.00821	0.00914	5	5	10
6	6	0.00634	0.00762	0.00708	0.00918	0.00706	0.00746	0.00706	0.00746	0.00429	0.00473	0.00543	0.00565	0.00621	0.00702	6	6	12

Higher intensity of colour means higher validity

Table 4 Obtained results of R^2 for several ANN (LM) models with different hidden nodes for the UB limit analysis method

Model number	Nodes in the hidden layer	Network result R^2 Iteration 1 TR1	TS1	Iteration 2 TR2	TS2	Iteration 3 TR3	TS3	Iteration 4 TR4	TS4	Iteration 5 TR5	TS5	Iteration 6 TR6	TS6	Average TR	TS	Average Ranking TR	TS	Total ranking
1	1	0.96800	0.97623	0.96836	0.97338	0.97382	0.96975	0.96884	0.97260	0.96885	0.97138	0.96877	0.97261	0.96944	0.97266	1	1	2
2	2	0.99587	0.99577	0.98827	0.98538	0.99101	0.99215	0.99584	0.99463	0.99052	0.98579	0.99646	0.99419	0.99300	0.99132	2	2	4
3	3	0.99550	0.99716	0.99851	0.99852	0.99814	0.99761	0.99867	0.99823	0.99855	0.99835	0.99823	0.99669	0.99793	0.99776	3	3	6
4	4	0.99925	0.99886	0.99934	0.99877	0.99881	0.99847	0.99863	0.99776	0.99904	0.99868	0.99830	0.99707	0.99890	0.99827	4	4	8
5	5	0.99961	0.99935	0.99896	0.99903	0.99915	0.99854	0.99940	0.99949	0.99955	0.99949	0.99970	0.99964	0.99939	0.99926	5	6	11
6	6	0.99964	0.99930	0.99965	0.99902	0.99934	0.99925	0.99954	0.99908	0.99944	0.99928	0.99962	0.99955	0.99954	0.99925	6	5	11

Higher intensity of colour means higher validity

Table 5 Obtained results of RMSE for 14 ANN (LM) models with different hidden nodes for the UB limit analysis method

Model number	Nodes in the hidden layer	Network result RMSE Iteration 1 TR1	TS1	Iteration 2 TR2	TS2	Iteration 3 TR3	TS3	Iteration 4 TR4	TS4	Iteration 5 TR5	TS5	Iteration 6 TR6	TS6	Average TR	TS	Average Ranking TR	TS	Total ranking
1	1	0.04576	0.04015	0.04494	0.04399	0.04494	0.04310	0.04494	0.04310	0.04503	0.04425	0.04448	0.04465	0.04502	0.04321	1	1	2
2	2	0.01647	0.01727	0.02812	0.03022	0.02642	0.02406	0.02642	0.02406	0.02559	0.02818	0.01564	0.01830	0.02311	0.02368	2	2	4
3	3	0.01691	0.01498	0.01004	0.01024	0.01256	0.01435	0.01256	0.01435	0.00975	0.01096	0.01126	0.01251	0.01218	0.01290	3	3	6
4	4	0.00720	0.00828	0.00678	0.00790	0.00907	0.00998	0.00907	0.00998	0.00814	0.00919	0.01041	0.01503	0.00844	0.01006	4	4	8
5	5	0.00520	0.00655	0.00833	0.00831	0.00829	0.00934	0.00829	0.00934	0.00542	0.00620	0.00446	0.00514	0.00667	0.00748	5	5	10
6	6	0.00481	0.00730	0.00500	0.00661	0.00706	0.00746	0.00706	0.00746	0.00621	0.00719	0.00503	0.00566	0.00586	0.00695	6	6	12

Higher intensity of colour means higher validity

The network performance R^2 and RMSE results changed based on the number of hidden nodes in each layer (e.g., Tables 2, 3 for the LB limit analysis and Tables 4, 5 for the UB limit analysis). Equations of RMSE and R^2 indices, model evaluation and total ranking used in this study can be found in other studies [60]. More details about the evaluation of the results obtained for the network performance (e.g., using the total ranking method) can be found in other studies (e.g., [61, 62]).

To propose an optimal architecture for the ANN predictive network, for the data obtained from the LB limit analysis, and based on the average R^2 and RMSE from all 72 constructed networks (e.g., including 6 iterations and from both testing and training datasets), model number 6, with 6 hidden neurons, showed better performance results (e.g., in regard to both R^2 and RMSE results) and could outperform the other 6 built models. The final ANN architecture that was selected for this model has a $3\times6\times1$ structure. Note that, the highest total ranking of 11 or 12 (e.g., again ranking the statistical indexes based on their performance results) was obtained for the model number 5 and 6, respectively. Sensitivity analysis for the R^2 after six iterations for the (a) LB limit analysis training datasets; (b) LB limit analysis testing datasets is presented in Fig. 5. Similarly, for the UB limit analysis, the R^2 after six iterations for the (a) UB limit analysis training datasets; (b) UB limit analysis testing datasets are provided in Fig. 6. On the other hand, having the UB limit analysis database, the optimal ANN architecture was obtained with the $3\times6\times1$ structure.

5.2 Hybrid ICA–ANN models predicting N_{2c}

In order to measure the applicability of proposed hybrid method results from an extensive number of limit equilibrium analysis (e.g., both UB and LB limit analysis) simulations were collected. These results were used in an optimized ANN training network (e.g., obtained from the previous section). The output of the ANN was then used for the ICA optimization algorithm as the input layer. All important network parameters of ICA were assessed using a trial-and-error process (e.g., number of countries, number of imperialists, and number of decades). Hence, in this step, the optimal structure of ICA–ANN was also achieved. Apart from this, to evaluate the capability of ANN and ICA–ANN methods total

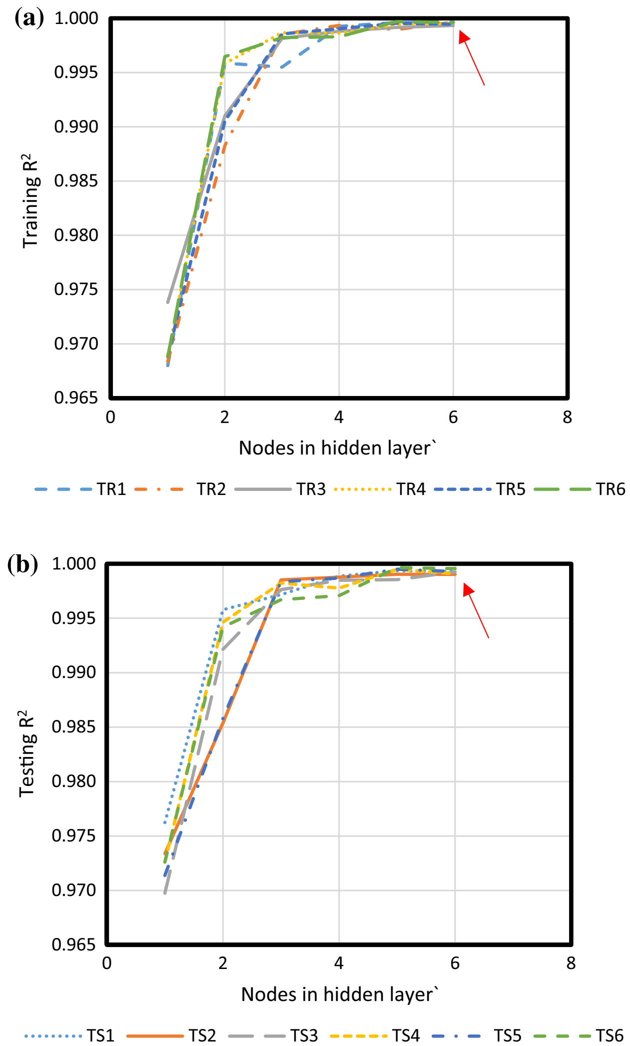

Fig. 5 R^2 sensitivity analysis after six ANN iterations for the **a** LB limit analysis training datasets; **b** LB limit analysis testing datasets

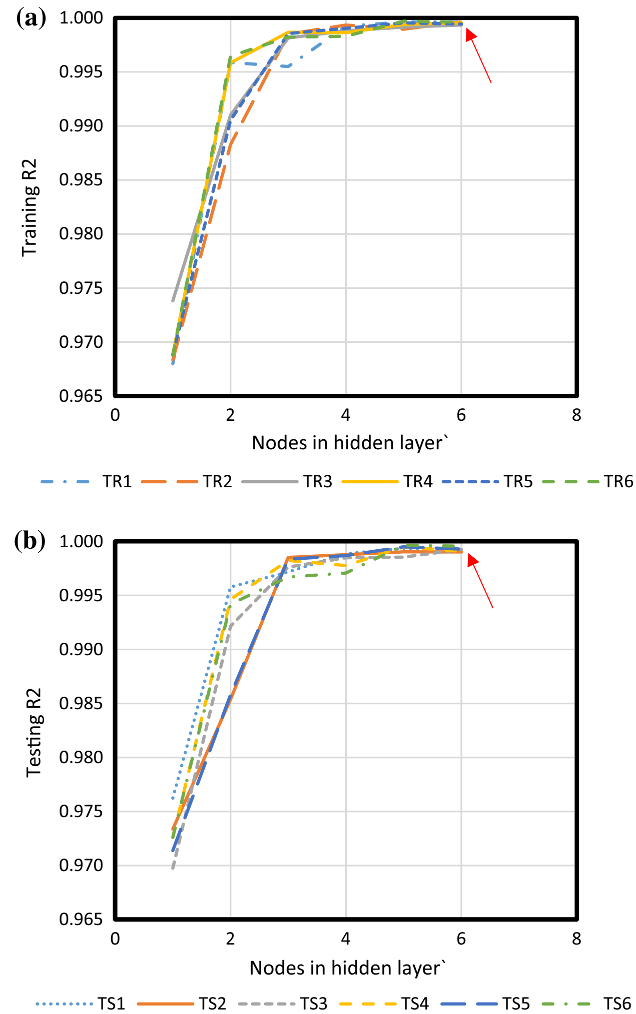

Fig. 6 R^2 sensitivity analysis after six ANN iterations for the **a** UB limit analysis training datasets; **b** UB limit analysis testing datasets

ranking system (TRS) and color intensity rating (CER) were used. These ranking methods were based on the obtained result from three statistical indices of R^2, RMSE, and VAF. These indices are well described in other studies (e.g., [1, 36, 63]). The performance results of ICA–ANN method for different values used for number of countries (e.g., 25, 50, 100, 150, 200, 250, 300, 350, 400 and 450), number of imperialists (e.g., 5, 10, 15, 20, 25, 30 and 35), and number of decades (50, 100, 150, 200, 250, 300, 400, 500 and 1000) for the LB and UB limit analysis method are assessed herein. TRS and CIR ranking systems for a different number of countries for the ICA–ANN–LB and ICA–ANN–UB limit analysis method are shown in Tables 6 and 7, respectively. Performance results for a different number of countries for the ICA–ANN–LB limit analysis and ICA–ANN–UB limit analysis methods are also presented in Figs. 7 and 8, respectively. Similarly, performance results for a different number of initial imperialists for the ICA–ANN–LB limit analysis and ICA–ANN–LB limit analysis method are shown in Figs. 9 and 10, respectively. From these figures, it can be concluded that for the LB and UB limit analysis, the ICA–ANN model with number of countries size equal to 350, number of imperialists equal to 10, and the number of decades equal to 200 leads to the best predictive network (e.g., for the ICA–ANN) model. Results from developed networks are provided for both testing and training datasets.

6 Model assessments

Based on the evaluation results, although both proposed models (e.g., ANN, ICA–ANN) have satisfactory approximation results in estimation stability number of N_{2c}, the hybrid ICA–ANN model can be presented as a more reliable and better simple non-linear ANN model in this field.

Table 6 TRS and CIR ranking systems for a different number of countries for the ICA–ANN–LB limit analysis method

Model number	Number of countries	Network result						Ranking						Total rank
		Train			Test			Train			Test			
		R^2	RMSE	VAF	R^2	RMSE	VAF	R^2	RMSE	VAF	R^2	RMSE	VAF	
1	25	0.9789	0.0389	99.9157	0.9672	0.0421	99.9663	3	3	3	2	2	2	15
2	50	0.9655	0.0519	99.8501	0.9424	0.0550	99.9425	1	1	1	1	1	1	6
3	75	0.9825	0.0357	99.9290	0.9733	0.0373	99.9736	5	5	5	5	5	5	30
4	100	0.9760	0.0419	99.9024	0.9729	0.0374	99.9735	2	2	2	4	4	4	18
5	150	0.9815	0.0366	99.9255	0.9697	0.0398	99.9698	4	4	4	3	3	3	21
6	200	0.9839	0.0341	99.9352	0.9850	0.0298	99.9831	6	6	6	7	7	7	39
7	250	0.9892	0.0284	99.9552	0.9871	0.0284	99.9846	11	11	11	10	9	9	61
8	300	0.9882	0.0294	99.9520	0.9855	0.0287	99.9843	10	10	10	8	8	8	54
9	350	0.9877	0.0296	99.9513	0.9856	0.0281	99.9850	9	9	9	9	10	10	56
10	400	0.9874	0.0302	99.9491	0.9880	0.0263	99.9869	8	8	8	11	11	11	57
11	450	0.9859	0.0317	99.9439	0.9821	0.0306	99.9822	7	7	7	6	6	6	39

Higher intensity of colour means higher validity

Table 7 TRS and CIR ranking systems for a different number of countries for the ICA–ANN–UB limit analysis method

Model number	Number of countries	Network result						Ranking						Total rank
		Train			Test			Train			Test			
		R^2	RMSE	VAF	R^2	RMSE	VAF	R^2	RMSE	VAF	R^2	RMSE	VAF	
1	25	0.9761	0.0397	99.8997	0.9839	0.0354	99.9842	1	1	1	4	6	7	20
2	50	0.9817	0.0341	99.9259	0.9844	0.0361	99.9835	6	5	5	6	4	5	31
3	75	0.9761	0.0390	99.9032	0.9793	0.0402	99.9796	2	2	2	1	1	1	9
4	100	0.9859	0.0302	99.9418	0.9886	0.0317	99.9873	10	10	11	10	9	10	60
5	150	0.9852	0.0305	99.9407	0.9880	0.0308	99.9880	9	9	10	9	10	11	58
6	200	0.9792	0.0359	99.9176	0.9853	0.0356	99.9840	4	4	4	7	5	6	30
7	250	0.9839	0.0316	99.9362	0.9864	0.0325	99.9866	8	8	8	8	8	9	49
8	300	0.9777	0.0375	99.9104	0.9811	0.0385	99.9813	3	3	3	2	2	3	16
9	350	0.9896	0.0254	99.9387	0.9933	0.0231	99.9800	11	11	9	11	11	2	55
10	400	0.9814	0.0340	99.9263	0.9828	0.0377	99.9821	5	6	6	3	3	4	27
11	450	0.9833	0.0323	99.9337	0.9842	0.0351	99.9844	7	7	7	5	7	8	41

Higher intensity of colour means higher validity

The learning process was acceptable in all predictive models. This could be clearly seen from high-performance results of both training and testing network. Based on R^2 and RMSE values of (0.9998 and 0.0017) and (0.9988 and 0.0018), respectively, were found for training and testing of the optimized ICA–ANN–LB predictive model. Similarly, for the ICA–ANN–UB predictive model, values of (0.9998, and 0.0017) and (0.9987 and 0.0019) were obtained for the R^2, and RMSE of training and testing datasets, respectively. However, in the optimal ANN model, the R^2 and RMSE for both of the training and testing datasets were (0.9993 and 0.00621) and (0.9992 and 0.00702), respectively. Note that, a high accuracy level of obtained network outputs from testing dataset indicates that the prediction result obtained from the developed network is reliable. Training and testing results of ANN model in predicting N_{2c} based on ANN predictive model (e.g., with 6 nodes for the LB and UB limit analysis) and ICA–ANN predictive models are presented in Figs. 11 and 12, respectively. Design charts using measured data from OptumG2 simulation, ANN–LB neural network analysis, ANN–UB neural network analysis, ICA–ANN–LB hybrid analysis, and ICA–ANN–UB hybrid analysis are presented in Figs. 13, 14, 15, 16 and 17.

7 Comparison of design solution charts

The results of design solution charts for both of the ANN and ICA–ANN predictive models are presented here. The predicted outputs obtained from the trained networks are compared with the results obtained from the finite element limit analysis (e.g., measured).These results are presented based on the comparison between actual with predicted values from both ANN and ICA analysis. Note that, to show a proper comparison between the ANN and ICA, the results from LB limit analysis were used. This is mainly because the result of R^2 in testing datasets was slightly higher. It can be seen that in both of the ANN outputs (e.g., as shown in Figs. 13, 14, 15, 16, 17 for $\beta = 15°$ to $\beta = 75°$, respectively) and ICA–ANN–LB (e.g., as shown in Figs. 18, 19, 20, 21,

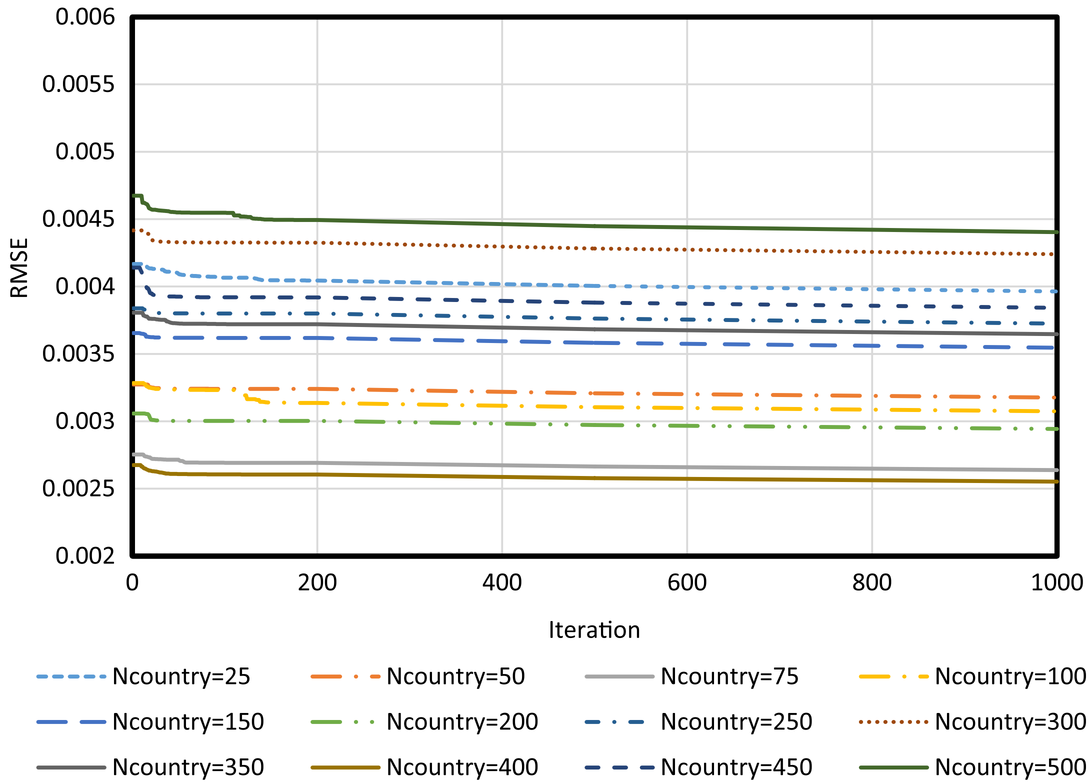

Fig. 7 performance results for a different number of countries for the ICA–ANN–LB limit analysis method

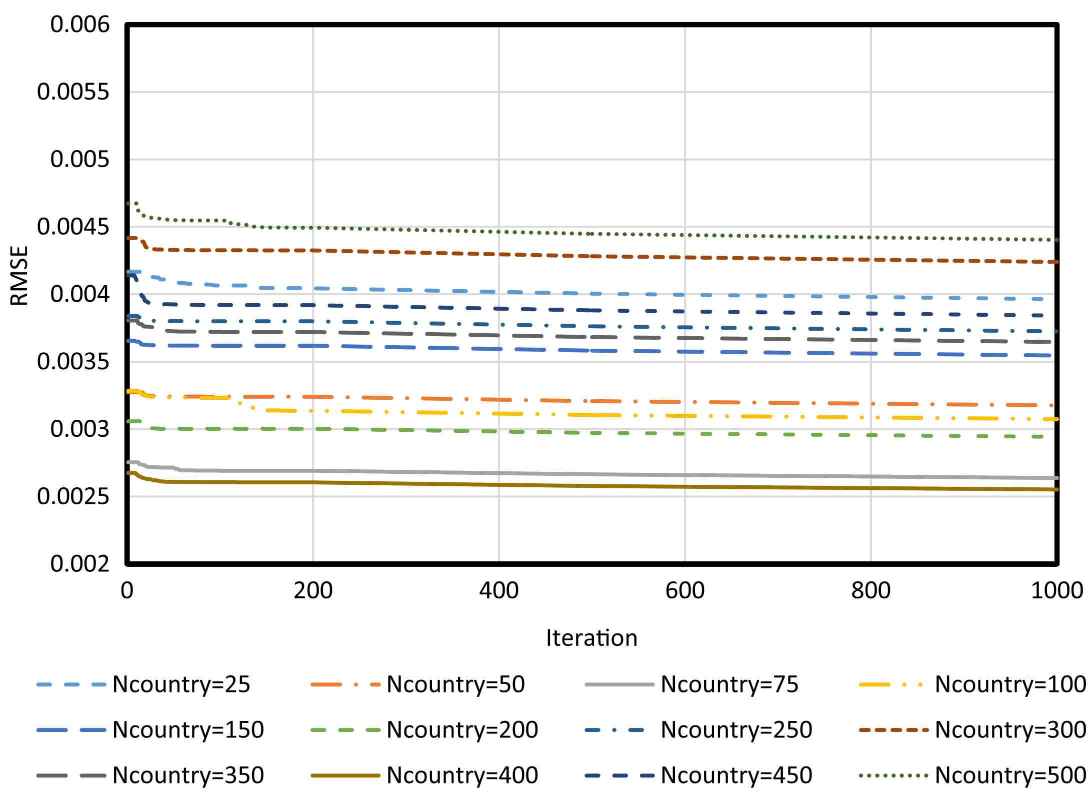

Fig. 8 Performance results for a different number of countries for the ICA–ANN–UB limit analysis method

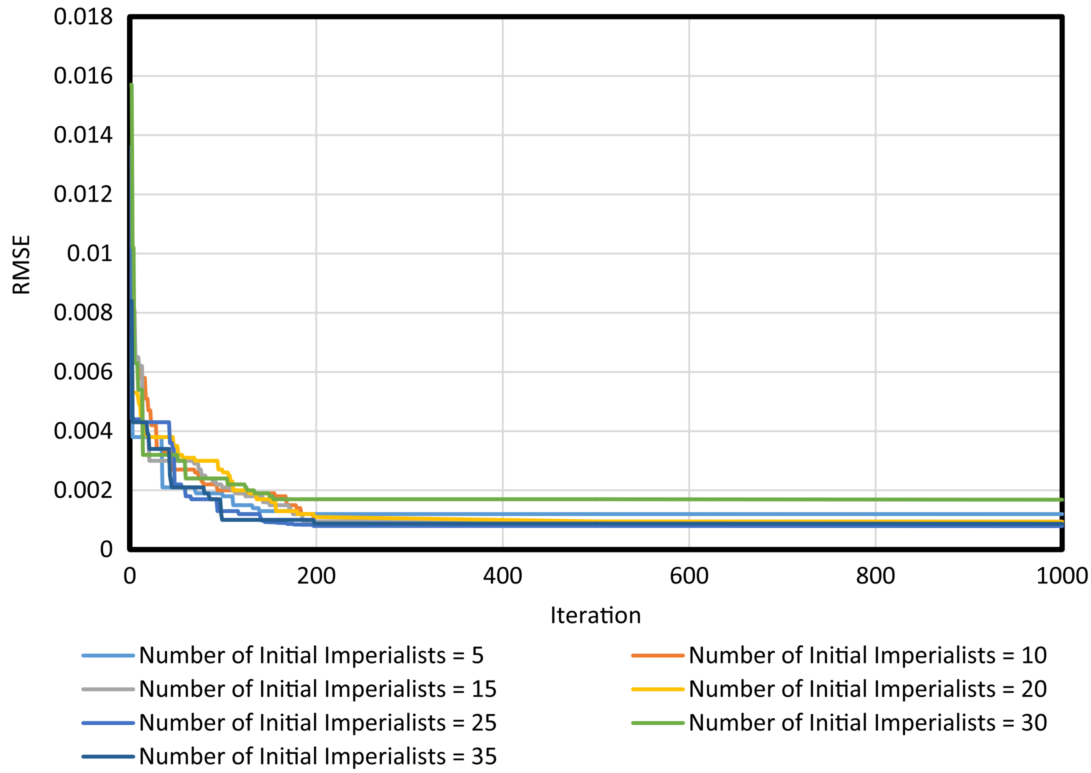

Fig. 9 Performance results for a different number of initial imperialists for the ICA–ANN–LB limit analysis method

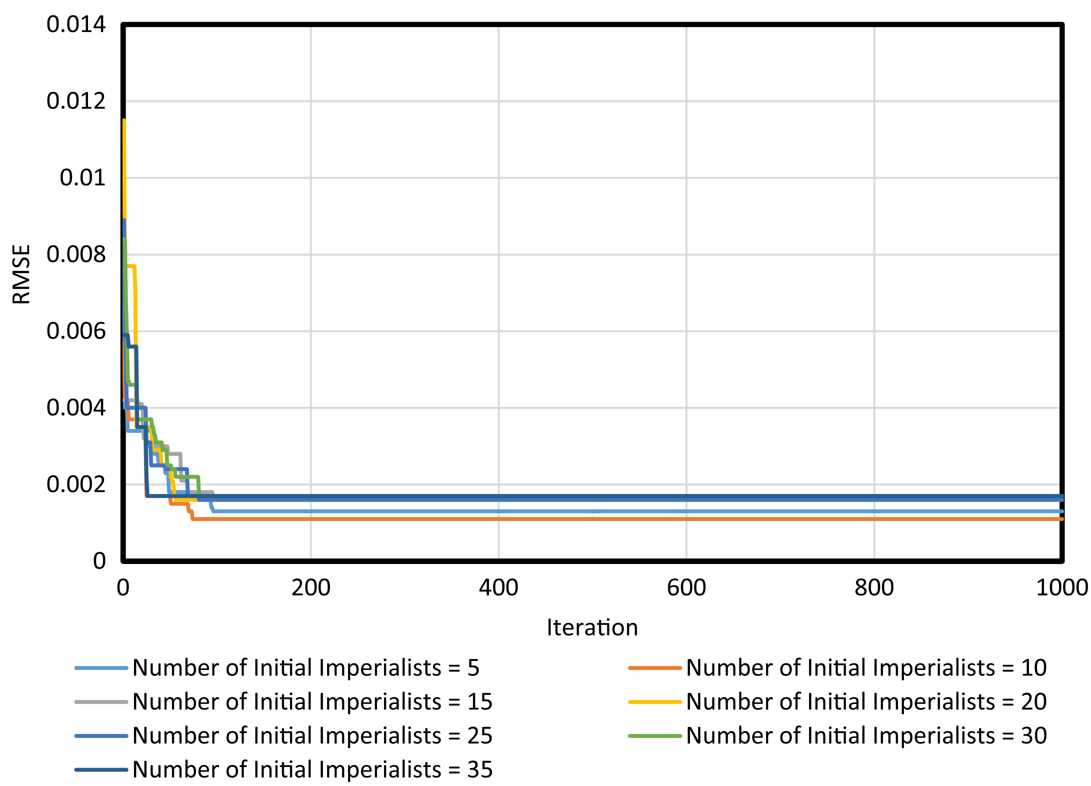

Fig. 10 Performance results for a different number of initial imperialists for the ICA–ANN–UB limit analysis method

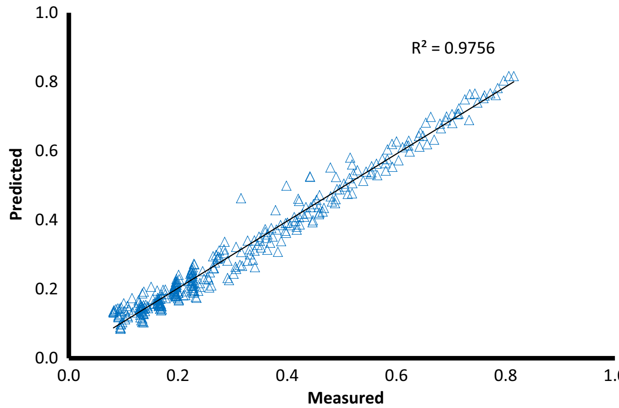

(a) LB training datasets

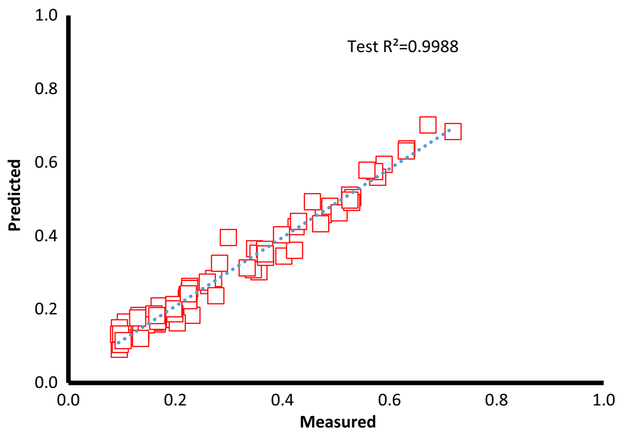

(b) LB testing datasets

Fig. 11 Training and testing results of optimized ICA–ANN model in predicting N_{2c} values of LB limit analysis method

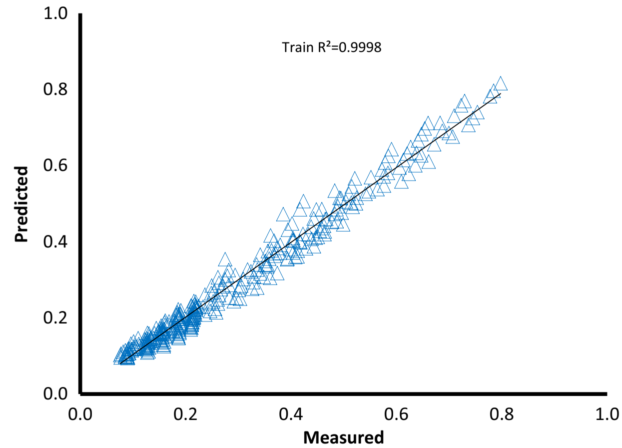

(a) UB Training datasets

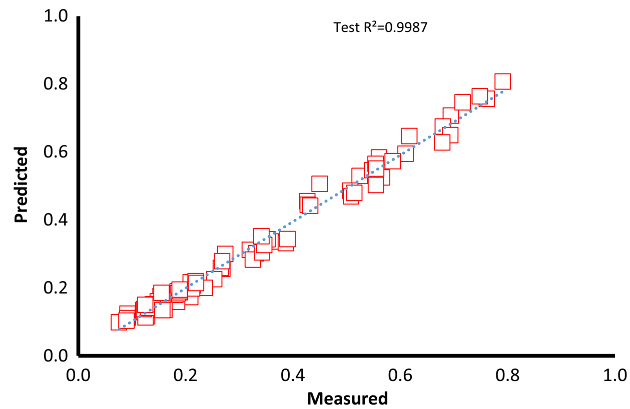

(b) UB Testing datasets

Fig. 12 Training and testing results of optimized ICA–ANN model in predicting N_{2c} values of UB limit analysis method

22 for $\beta = 15°$ to $\beta = 75°$, respectively) analysis, the result obtained from ICA–ANN trained network is more accurate than a simple ANN model. Also, the result of the design solution charts is provided only for the LB limit analysis as this was only an example of the solutions provided by the ICA–ANN hybrid model showing its superiority to simple ANN technique.

8 Conclusions

This study aimed to propose a new hybrid ICA–ANN predictive model in order to provide design solution charts for the cohesive slopes. First, after a trial-and-error process (e.g., with 72 different ANN architectures) a proper structure for the optimal ANN model was presented. The established database and ANN modeling procedures were developed and finally, the obtained results from each introduced technique (e.g., ANN and ICA–ANN) compared and the effect of their most influential parameters was observed. Next, the ICA–ANN methods were optimized using a trial-and-error process (e.g., by changing their most influential parameters such as the number of countries, number of imperialists and number of decades). TRS and CER were used to evaluate the applicability of the presented method. These ranking techniques were conducted based on the result of three statistical indices namely, R^2, RMSE, and VAF. The obtained results proved that the hybrid ICA–ANN model (e.g., in its optimal conditions that obtained in this study) could be proposed as a better and more reliable ANN model, in the estimation of slope stability factor of safety, compared to ANN model. From high-performance results of the trained network, it can be concluded that the learning process was acceptable. In the optimal ANN of the LB and UB limit analysis models, the R^2 and RMSE were (0.9994 and 0.00621) and (0.9995 and 0.00586) for the training datasets and (0.9993 and 0.00702) and (0.9992 and 0.00695) for the testing datasets, respectively. However, according to the ICA–ANN method of LB and UB limit analysis, values of (0.9998, and 0.0017) and (0.9998 and 0.0017), respectively, were found for R^2 and RMSE of training datasets and (0.9988 and 0.0018) and

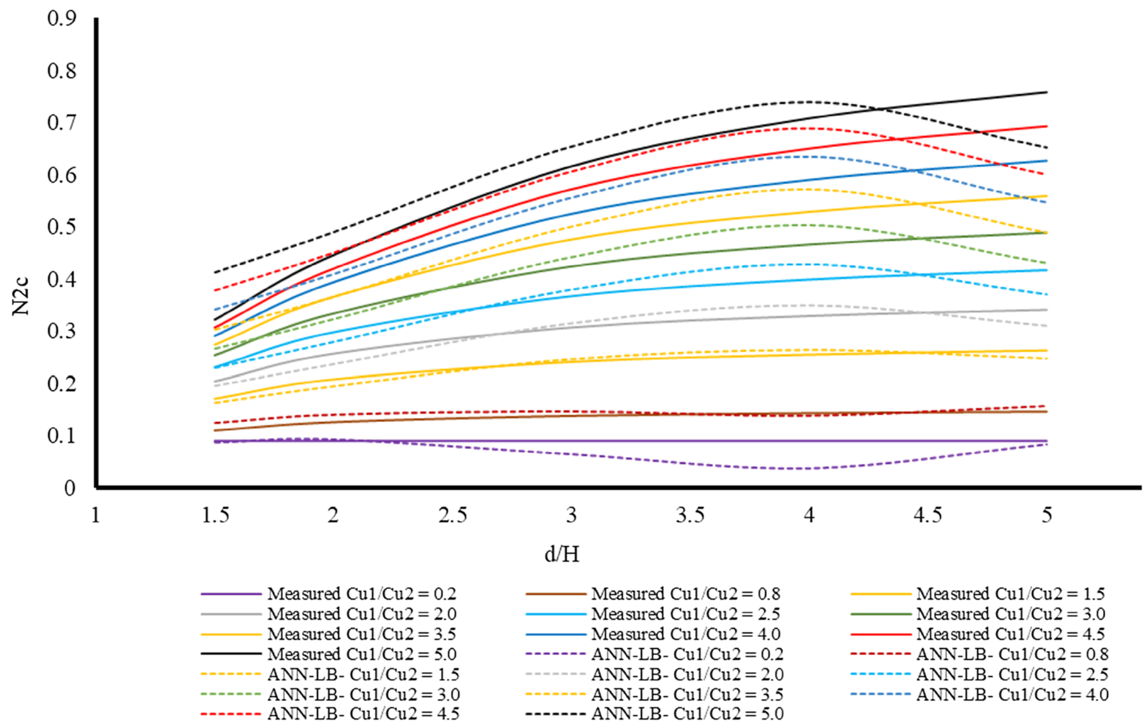

Fig. 13 Results of ANN–LB limit analysis for measured and predicted N_{2c} in slope with $\beta = 15°$

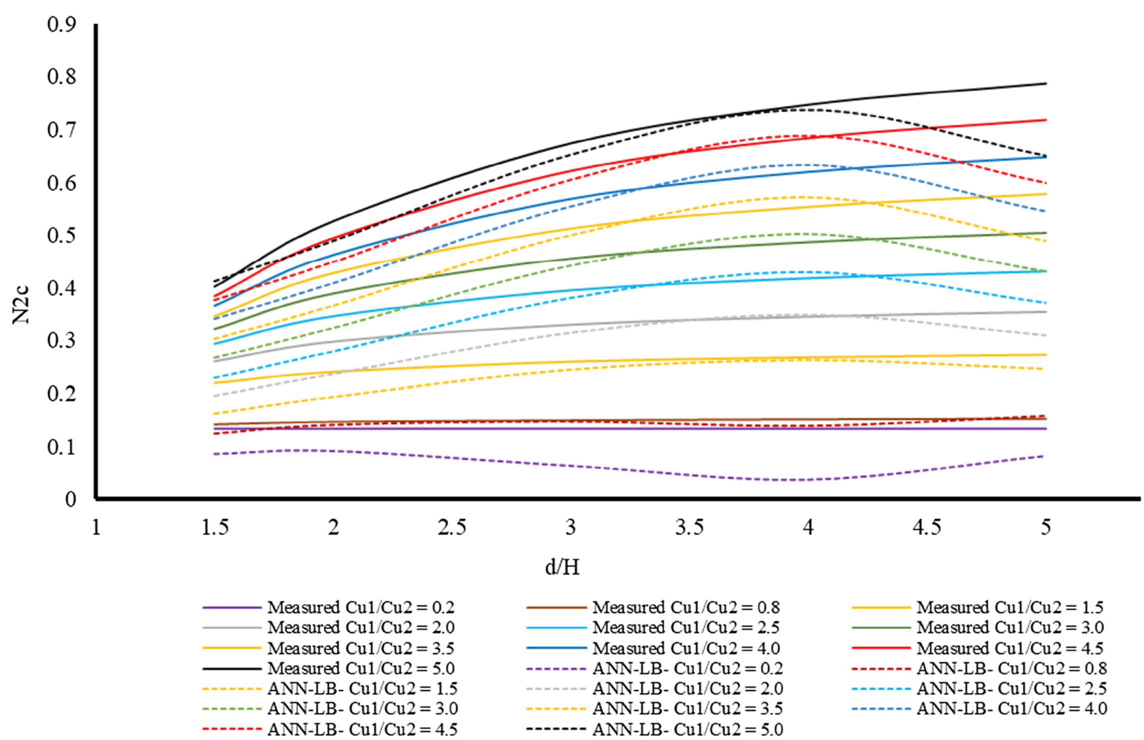

Fig. 14 Results of ANN–LB limit analysis for measured and predicted N_{2c} in slope with $\beta = 30°$

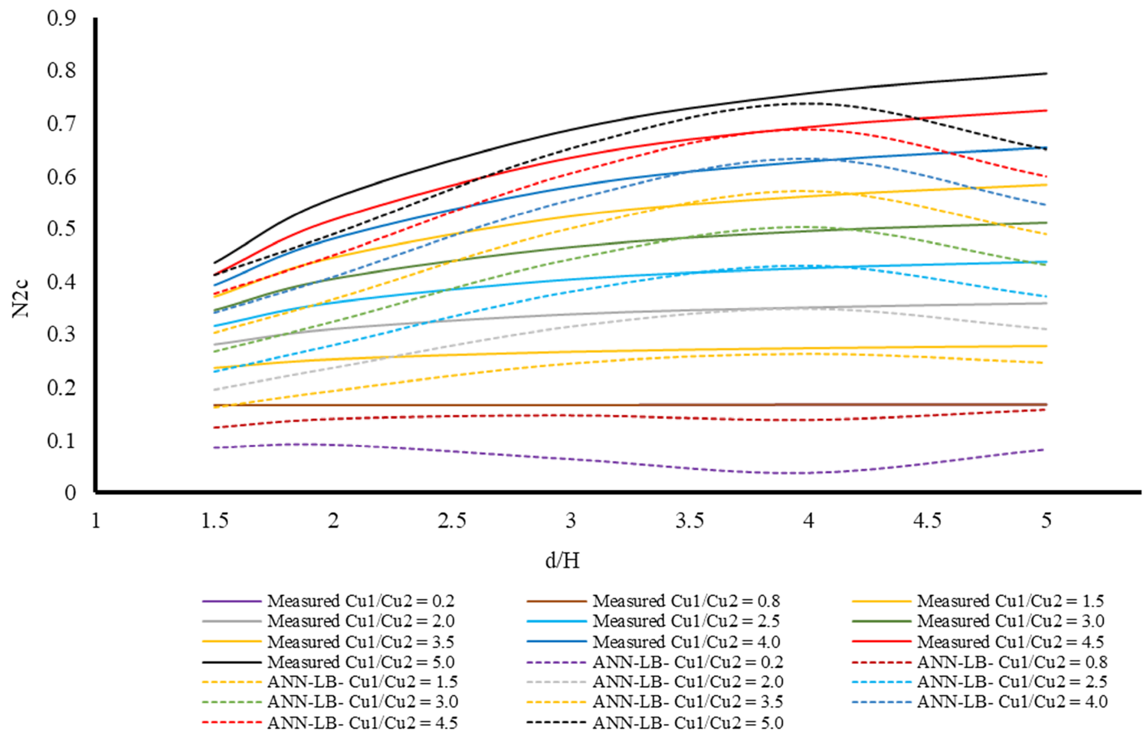

Fig. 15 Results of ANN–LB limit analysis for measured and predicted N_{2c} in slope with $\beta = 45°$

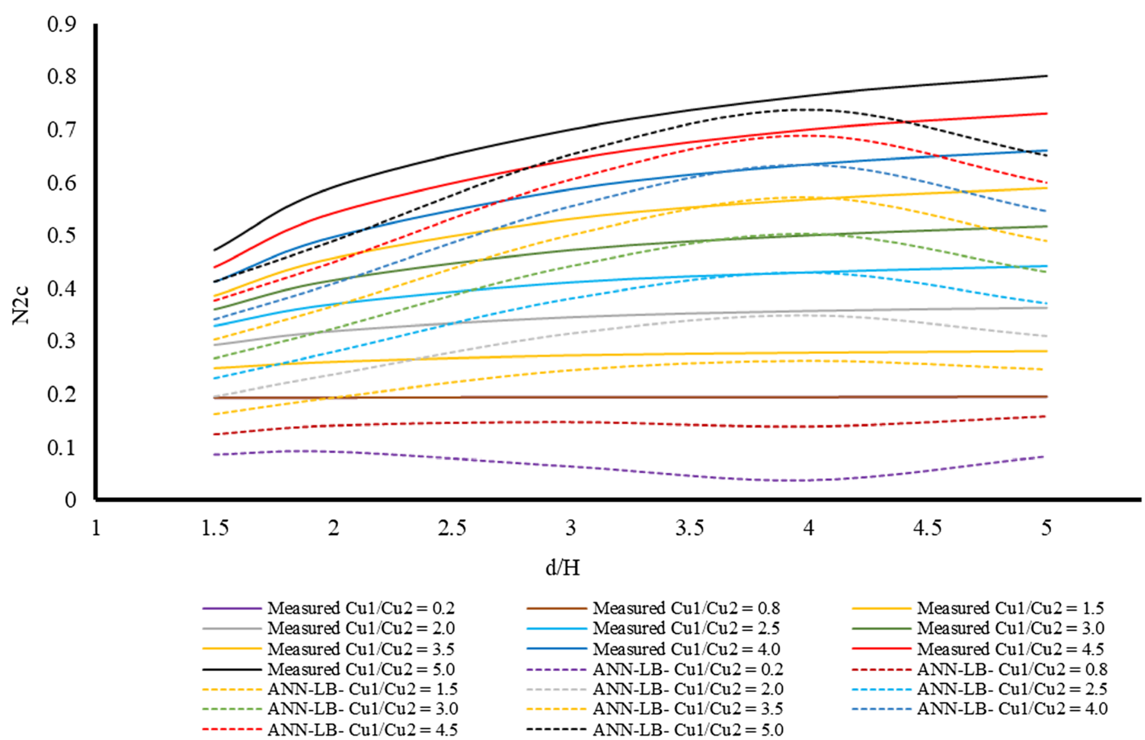

Fig. 16 Results of ANN–LB limit analysis for measured and predicted N_{2c} in slope with $\beta = 60°$

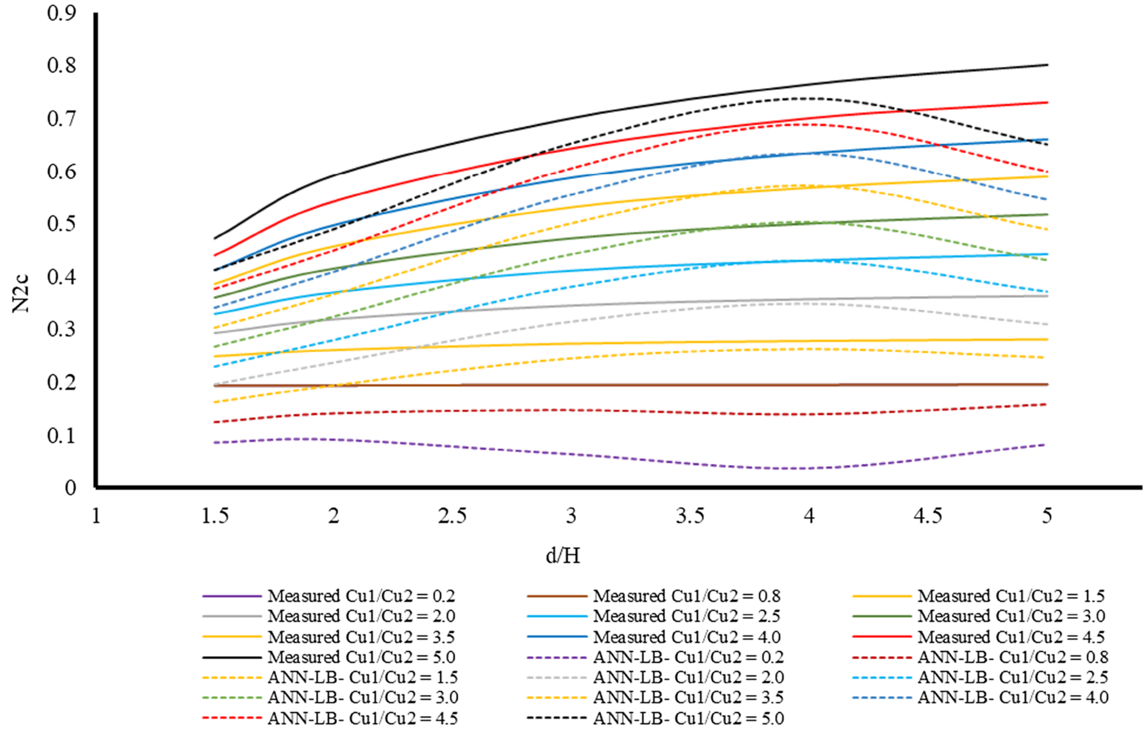

Fig. 17 Results of ANN–LB limit analysis for measured and predicted N_{2c} in slope with $\beta = 75°$

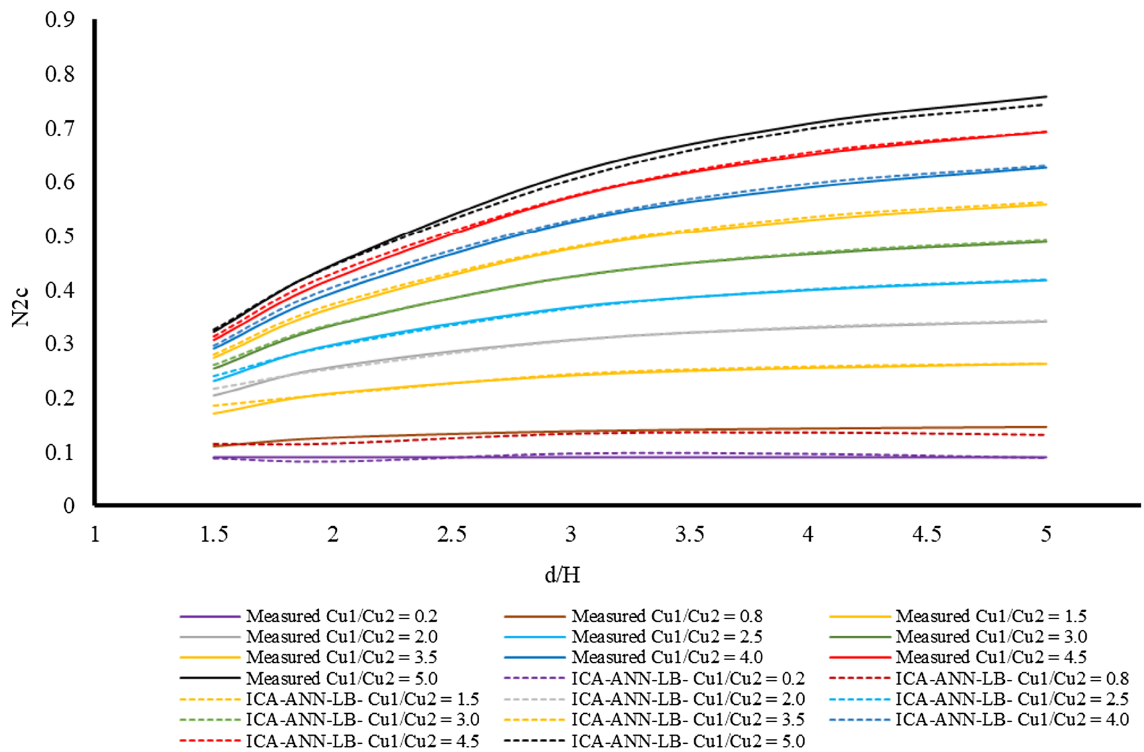

Fig. 18 Results of ICA–ANN–LB limit analysis for measured and predicted N_{2c} in slope with $\beta = 15°$

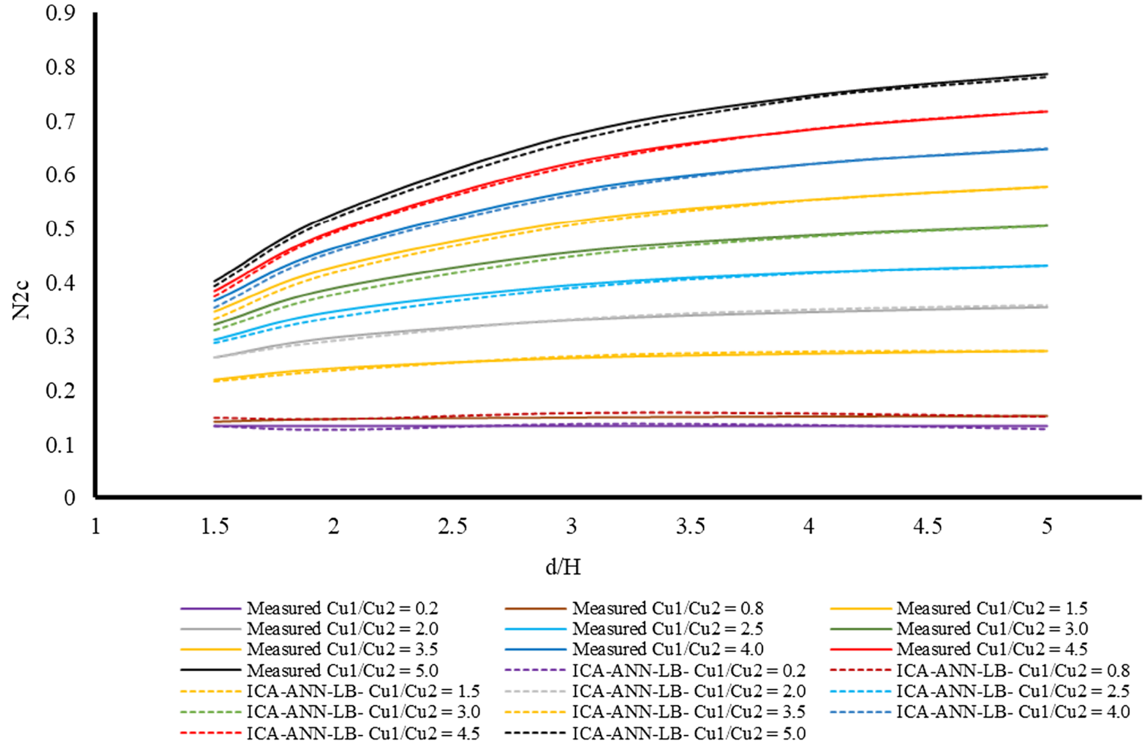

Fig. 19 Results of ICA–ANN–LB limit analysis for measured and predicted N_{2c} in slope with $\beta = 30°$

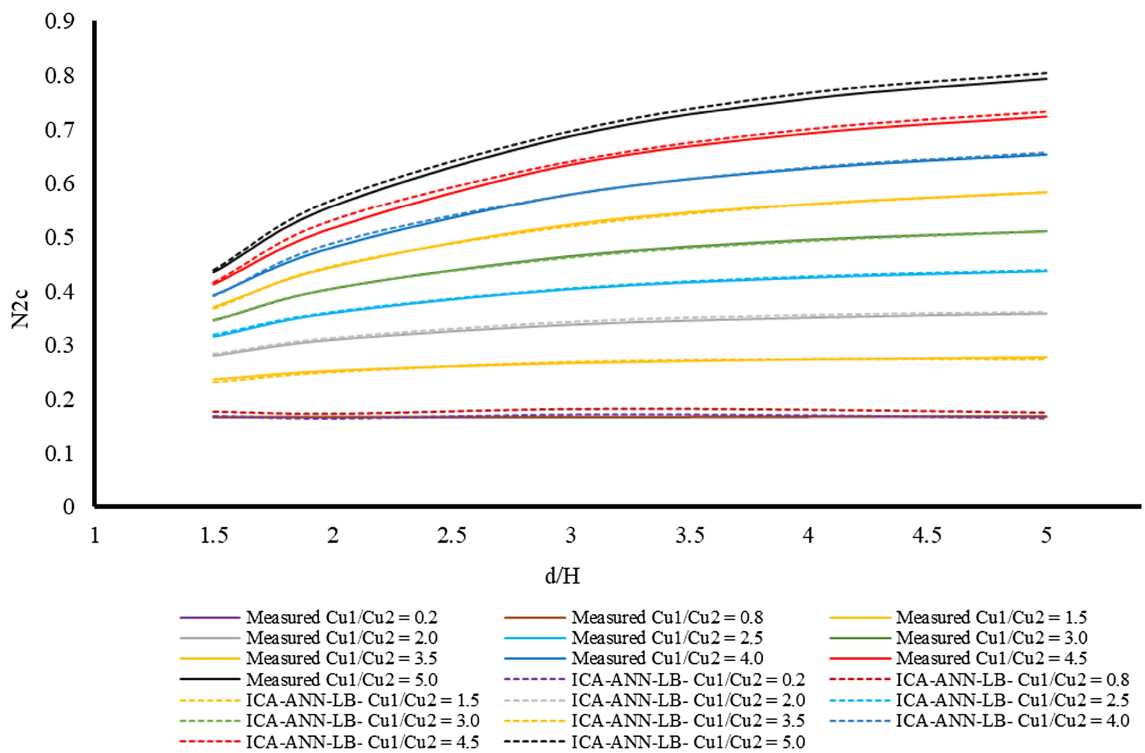

Fig. 20 Results of ICA–ANN–LB limit analysis for measured and predicted N_{2c} in slope with $\beta = 45°$

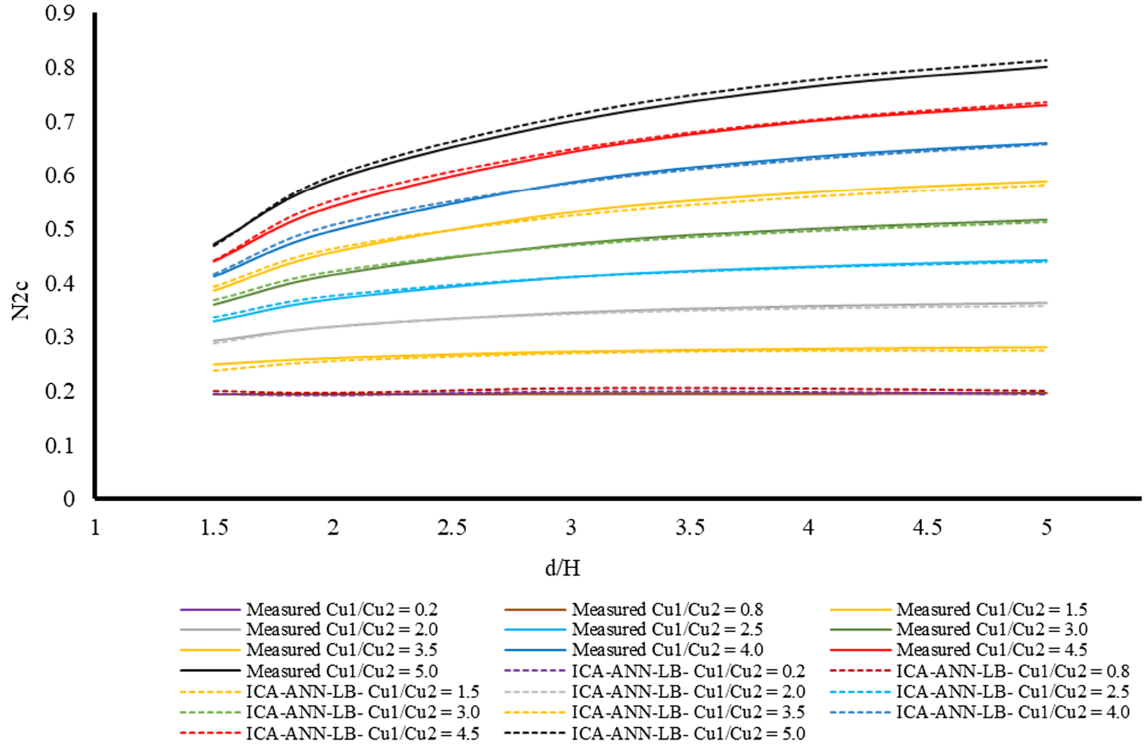

Fig. 21 Results of ICA–ANN–LB limit analysis for measured and predicted N_{2c} in slope with $\beta = 60°$

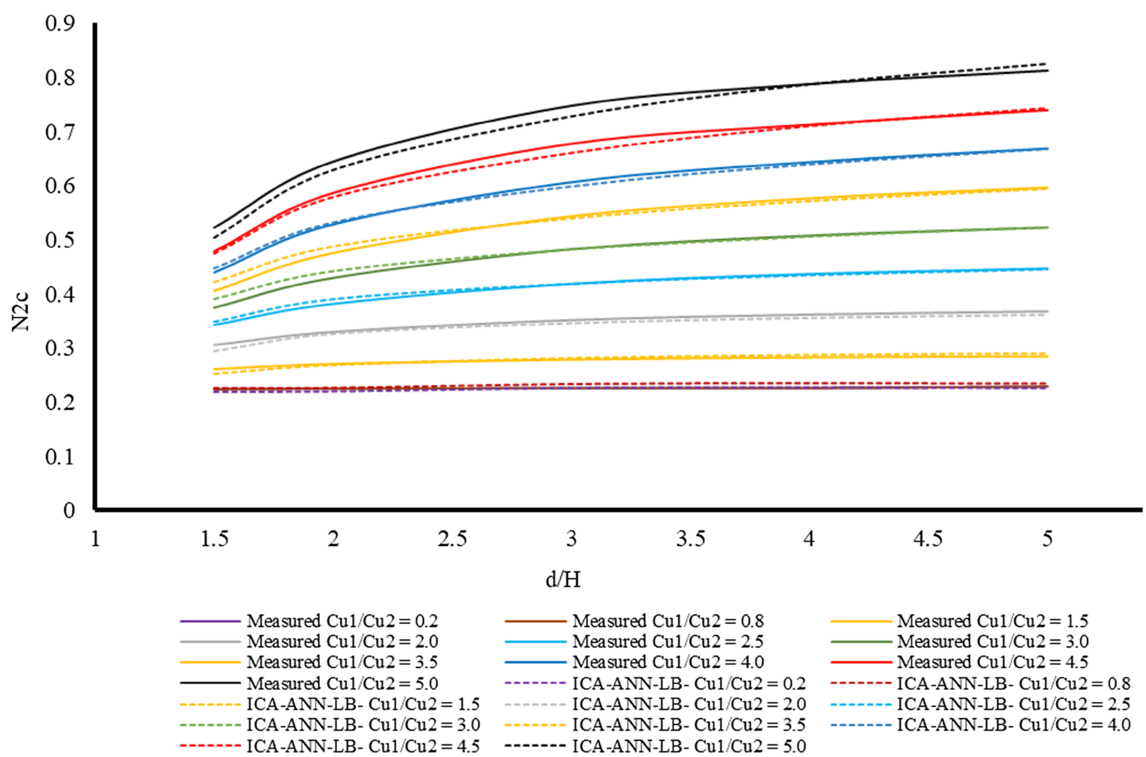

Fig. 22 Results of ICA–ANN–LB limit analysis for measured and predicted N_{2c} in slope with $\beta = 75°$

(0.9987 and 0.0019) for the testing datasets of the optimized ICA–ANN–LB predictive model, respectively. From both presented predictive models, i.e., to predict the slope stability a dimensionless number of the cohesive slope, the ICA–ANN predictive model can provide lower RMSE and higher R^2 (i.e., higher network performance) in terms of introduced statistical indexes for both training and testing phases compared to simple ANN method.

Compliance with ethical standards

Conflict of interest The authors declare no conflict of interest.

References

1. Koopialipoor M, Armaghani DJ, Hedayat A, Marto A, Gordan B (2018) Applying various hybrid intelligent systems to evaluate and predict slope stability under static and dynamic conditions. Soft Comput 23:1–17
2. Marrapu BM, Jakka RS (2017) Assessment of slope stability using multiple regression analysis. Geomech Eng 13:237–254
3. Nazir R, Ghareh S, Mosallanezhad M, Moayedi H (2016) The influence of rainfall intensity on soil loss mass from cellular confined slopes. Measurement 81:13–25
4. Li AJ, Khoo SY, Wang Y, Lyamin AV (2014) Application of neural network to rock slope stability assessments. CRC Press-Taylor & Francis Group, Boca Raton
5. Moayedi H, Huat BB, Mohammad Ali TA, Asadi A, Moayedi F, Mokhberi M (2011) Preventing landslides in times of rainfall: case study and FEM analyses. Disaster Prev Manag Int J 20:115–124
6. Niroumand H, Kassim KA, Nazir R, Faizi K, Adhami B, Moayedi H, Loon W (2012) Slope stability and sheet pile and contiguous bored pile walls. Electron J Geotech Eng 17:19–27
7. Raftari M, Kassim KA, Rashid ASA, Moayedi H (2013) Settlement of shallow foundations near reinforced slopes. Electron J Geotech Eng 18:797–808
8. Latifi N, Horpibulsuk S, Meehan CL, Abd Majid MZ, Tahir MM, Mohamad ET (2016) Improvement of problematic soils with biopolymer—an environmentally friendly soil stabilizer. J Mater Civ Eng. https://doi.org/10.1061/(ASCE)MT.1943-5533.0001706
9. Moayedi H, Huat BB, Asadi A (2010) Strain absorption optimization of reinforcement in geosynthetic reinforced slope-experimental and FEM modeling. Electron J Geotech Eng 15:1563–1569
10. Nazir R, Moayedi H (2014) Soil mass loss reduction during rainfalls by reinforcing the slopes with the surficial confinement. Int J Geol Environ Eng 8(6):381–384
11. Moayedi H, Huat B, Kazemian S, Asadi A (2010) Optimization of shear behavior of reinforcement through the reinforced slope. Electron J Geotech Eng 15:93–104
12. Georgiadis K (2010) Undrained bearing capacity of strip footings on slopes. J Geotech Geoenviron Eng 136:677–685
13. Moayedi H, Huat BBK, Kazemian S, Asadi A (2010) Optimization of tension absorption of geosynthetics through reinforced slope. Electron J Geotech Eng 15:93–104
14. Taylor DW (1937) Stability of earth slopes. J Boston Soc Civ Eng 24:197–246
15. Basarir H, Kumral M, Karpuz C, Tutluoglu L (2010) Geostatistical modeling of spatial variability of SPT data for a borax stockpile site. Eng Geol 114:154–163
16. Alnaqi AA, Moayedi H, Shahsavar A, Nguyen TK (2019) Prediction of energetic performance of a building integrated photovoltaic/thermal system thorough artificial neural network and hybrid particle swarm optimization models. Energy Convers Manag 183:137–148
17. Shahsavar A, Khanmohammadi S, Khaki M, Salmanzadeh M (2018) Performance assessment of an innovative exhaust air energy recovery system based on the PV/T-assisted thermal wheel. Energy 162:682–696
18. Shahsavar A, Salmanzadeh M, Ameri M, Talebizadeh P (2011) Energy saving in buildings by using the exhaust and ventilation air for cooling of photovoltaic panels. Energy Build 43:2219–2226
19. Mohamad ET, Armaghani DJ, Momeni E, Yazdavar AH, Ebrahimi M (2016) Rock strength estimation: a PSO-based BP approach. Neural Comput Appl 1–12
20. Asadi A, Moayedi H, Huat BB, Boroujeni FZ, Parsaie A, Sojoudi S (2011) Prediction of zeta potential for tropical peat in the presence of different cations using artificial neural networks. Int J Electrochem Sci 6:1146–1158
21. Asadi A, Moayedi H, Huat BBK, Parsaie A, Taha MR (2011) Artificial neural networks approach for electrochemical resistivity of highly organic soil. Int J Electrochem Sci 6:1135–1145
22. Mohamad ET, Faradonbeh RS, Armaghani DJ, Monjezi M, Majid MZA (2017) An optimized ANN model based on genetic algorithm for predicting ripping production. Neural Comput Appl 28:393–406
23. Armaghani DJ, Hasanipanah M, Mahdiyar A, Majid MZA, Amnieh HB, Tahir M (2018) Airblast prediction through a hybrid genetic algorithm-ANN model. Neural Comput Appl 29:619–629
24. Hasanipanah M, Noorian-Bidgoli M, Armaghani DJ, Khamesi H (2016) Feasibility of PSO-ANN model for predicting surface settlement caused by tunneling. Eng Comput 32:705–715
25. Li J, Wang J (2010) Research of steel plate temperature prediction based on the improved PSO-ANN algorithm for Roller Hearth Normalizing Furnace. In: 2010 8th World congress on intelligent control and automation (WCICA), pp 2464–2469
26. Marzband M, Parhizi N, Adabi J (2016) Optimal energy management for stand-alone microgrids based on multi-period imperialist competition algorithm considering uncertainties: experimental validation. Int Trans Electr Energy Syst 26:1358–1372
27. Choobbasti AJ, Farrokhzad F, Barari A (2009) Prediction of slope stability using artificial neural network (case study: Noabad, Mazandaran, Iran). Arab J Geosci 2:311–319
28. Su GS, Zhang Y, Chen GQ, Yan LB (2013) Fast estimation of slope stability based on gaussian process machine learning. Disaster Adv 6:81–91
29. Chakraborty A, Goswami D (2017) Prediction of slope stability using multiple linear regression (MLR) and artificial neural network (ANN). Arab J Geosci 10:11
30. Cheng YM, Lansivaara T, Baker R, Li N (2013) Use of internal and external variables and extremum principle in limit equilibrium formulations with application to bearing capacity and slope stability problems. Soils Found 53:130–143
31. Zhang ZF, Liu ZB, Zheng LF, Zhang Y (2014) Development of an adaptive relevance vector machine approach for slope stability inference. Neural Comput Appl 25:2025–2035
32. Donald IB, Chen Z (1997) Slope stability analysis by the upper bound approach: fundamentals and methods. Can Geotech J 34:853–862
33. Niroumand H, Faizi K, Nazir R, Kassin K, Moayedi H (2012) Slope stability of the design concept of the sheet pile and contiguous bored pile walls. Arch Des Sci 65:2–17
34. Kostic S, Vasovic N, Todorovic K, Samcovic A (2016) Application of artificial neural networks for slope stability analysis in geotechnical practice. In: 2016 13th Symposium on neural networks and applications (Neural), pp 89–94

35. McCulloch W, Pitts W (1943) A logical calculus of the ideas immanent in nervous activity. Bull Math Biophys 5:115–133
36. Mosallanezhad M, Moayedi H (2017) Developing hybrid artificial neural network model for predicting uplift resistance of screw piles. Arab J Geosci 10:10
37. Gandomi AH, Alavi AH (2012) A new multi-gene genetic programming approach to non-linear system modeling. Part II: geotechnical and earthquake engineering problems. Neural Comput Appl 21:189–201
38. Moayedi H, Hayati S (2018) Artificial intelligence design charts for predicting friction capacity of driven pile in clay. Neural Comput Appl. https://doi.org/10.1007/s00521-018-3555-5
39. Al Dossary MA, Nasrabadi H (2016) Well placement optimization using imperialist competitive algorithm. J Pet Sci Eng 147:237–248
40. Atashpaz-Gargari E, Lucas C (2007) Imperialist competitive algorithm: an algorithm for optimization inspired by imperialistic competition. IEEE
41. Soleimani S, Jiao PC, Rajaei S, Forsati R (2018) A new approach for prediction of collapse settlement of sandy gravel soils. Eng Comput 34:15–24
42. Moayedi H, Armaghani DJ (2018) Optimizing an ANN model with ICA for estimating bearing capacity of driven pile in cohesionless soil. Eng Comput 34:347–356. https://doi.org/10.1007/s00366-017-0545-7
43. Sloan SW (1988) Lower bound limit analysis using finite elements and linear programming. Int J Numer Anal Meth Geomech 12:61–77
44. Zhou J, Chen Q, Wang J (2017) Rigid block based lower bound limit analysis method for stability analysis of fractured rock mass considering rock bridge effects. Comput Geotech 86:173–180
45. Lim K, Li A, Lyamin A (2015) Three-dimensional slope stability assessment of two-layered undrained clay. Comput Geotech 70:1–17
46. Chen Z, Wang X, Haberfield C, Yin J-H, Wang Y (2001) A three-dimensional slope stability analysis method using the upper bound theorem: part I: theory and methods. Int J Rock Mech Min Sci 38:369–378
47. Chen J, Yin J-H, Lee CF (2003) Upper bound limit analysis of slope stability using rigid finite elements and nonlinear programming. Can Geotech J 40:742–752
48. Zhao L-h, Li L, Yang F, Luo Q, Liu X (2010) Upper bound analysis of slope stability with nonlinear failure criterion based on strength reduction technique. J Cent South Univ Technol 17:836–844
49. Krabbenhoft K, Lyamin A, Krabbenhoft J (2015) Optum computational engineering (OptumG2). Computer software. https://www.optumce.com (Software accessed since 2013)
50. Caër T, Souloumiac P, Maillot B, Leturmy P, Nussbaum C (2018) Propagation of a fold-and-thrust belt over a basement graben. J Struct Geol 115:121–131
51. Zhou H, Liu H, Yin F, Chu J (2018) Upper and lower bound solutions for pressure-controlled cylindrical and spherical cavity expansion in semi-infinite soil. Comput Geotech 103:93–102
52. Karkanaki AR, Ganjian N, Askari F (2017) Stability analysis and design of cantilever retaining walls with regard to possible failure mechanisms: an upper bound limit analysis approach. Geotech Geol Eng 35:1079–1092
53. Mahdiyar A, Hasanipanah M, Armaghani DJ, Gordan B, Abdullah A, Arab H, Abd Majid MZ (2017) A Monte Carlo technique in safety assessment of slope under seismic condition. Eng Comput 33:807–817
54. Yusof MF, Azamathulla HM, Abdullah R (2014) Prediction of soil erodibility factor for Peninsular Malaysia soil series using ANN. Neural Comput Appl 24:383–389
55. Siddiqui FI, Pathan DM, Osman S, Pinjaro MA, Memon S (2015) Comparison between regression and ANN models for relationship of soil properties and electrical resistivity. Arab J Geosci 8:6145–6155
56. Verma AK, Kishore K, Chatterjee S (2016) Prediction model of longwall powered support capacity using field monitored data of a longwall panel and uncertainty-based neural network. Geotech Geol Eng 34:2033–2052
57. Rana MJ, Shahriar MS, Shafiullah M (2017) Levenberg–Marquardt neural network to estimate UPFC-coordinated PSS parameters to enhance power system stability. Neural Comput Appl 1–12
58. Wang C (1994) A theory of generalization in learning machines with neural application. The University of Pennsylvania, Philadelphia
59. Sharma LK, Vishal V, Singh TN (2017) Developing novel models using neural networks and fuzzy systems for the prediction of strength of rocks from key geomechanical properties. Measurement 102:158–169
60. Gupta R, Goyal K, Yadav N (2016) Prediction of safe bearing capacity of noncohesive soil in arid zone using artificial neural networks. Int J Geomech 16:7
61. Moayedi H, Rezaei A (2017) an artificial neural network approach for under reamed piles subjected to uplift forces in dry sand. Neural Comput Appl 28:1–10
62. Moayedi H, Hayati S (2018) Modelling and optimization of ultimate bearing capacity of strip footing near a slope by soft computing methods. Appl Soft Comput 66:208–219
63. Moayedi H, Hayati S (2018) Applicability of a CPT-based neural network solution in predicting load-settlement responses of bored pile. Int J Geomech 18:06018009

Publisher's Note Springer Nature remains neutral with regard to jurisdictional claims in published maps and institutional affiliations.